

Focusing in dip and AVA compensation on scattering-angle/azimuth common image gathers

Sverre Brandsberg-Dahl[†], Maarten V. de Hoop[†] and Bjørn Ursin^{††}

[†] Center for Wave Phenomena, Colorado School of Mines, Golden, CO 80401 USA.

^{††}Department of petroleum technology and applied geophysics, NTNU, N-7491 Trondheim, Norway.

Abstract

Common image gathers (CIGs) in the offset and surface azimuth domain are used extensively in migration velocity analysis and amplitude versus offset (AVO) studies. If the geology is complex and the rayfield becomes multi-pathed, the quality of the CIGs deteriorates. To overcome these problems, the CIGs are instead generated as a function of scattering-angle and azimuth at the image point. These CIGs are generated using an algorithm based on the inverse generalized Radon transform (GRT), but stacking only over migration dip angles. Including only dips in the vicinity of the geological dip, or focusing in dip, results in improved signal-to-noise ratio on the CIGs because only the essential data points are used.

Introduction

If the geology is complex and the rayfield becomes multi-pathed, the assumptions made for imaging data in the offset domain are violated. This will especially influence the quality of image gathers, and hence make it difficult to perform any form of amplitude versus angle (AVA) or differential semblance based migration velocity analysis. In an effort to overcome these problems we present a novel parameterization of such image gathers, where we replace the offset parameter with scattering angle. This is based on the natural parameterization of rays at the scattering point: takeoff directions or alternatively migration-dip, scattering-angle and azimuth: *angles parameterization*. The resulting common image gathers (CIGs) are parametrized in space coordinates and scattering-angle/azimuth. By using the angle parametrization, we unravel the multi-pathing and get a correct representation of the redundancy in the wavefront set of the data. The angle CIGs can be used directly for AVA (Castagna & Backus, 1993), they can provide information about the medium parameters (Ursin *et al.*, 1996), and they will be well suited for use in migration velocity analysis (Jeannot *et al.*, 1986). Also, the occurrence of migration dip in the parametrization allows us to estimate the local geological dip, a procedure which we call ‘focusing in dip’. This focusing procedure also enhances the signal-to-noise ratio in both the gathers and the stacked images. When used in velocity analysis we remove the AVA effects from the CIGs in the background medium, and the CIGs will, depending on the current background medium, have a uniform signature in the reconstructed perturbation. Any residual moveout or AVA effects in the gathers can then be related to errors in this background model. The theory is developed for heterogeneous, anisotropic media while the present application is for isotropic media.

Basic equations

We consider wave propagation in an inhomogeneous anisotropic solid. The wave equation in the frequency domain is $\omega^2 \rho G_{in} + \partial_j (c_{ijkl} \partial_l G_{kn}) = -\delta_{in} \delta(\mathbf{x} - \mathbf{x}')$. Here the Green’s tensor $G_{in}(\mathbf{x}, \mathbf{x}', \omega)$ is the displacement in the x_i direction at the point $\mathbf{x} = (x_1, x_2, x_3)$ due to a point source in the x_n direction at the source position $\mathbf{x}' = (x'_1, x'_2, x'_3)$, $\rho(\mathbf{x})$ is the density and $c_{ijkl}(\mathbf{x})$ represents the elastic stiffness tensor at the point \mathbf{x} . We assume that the parameters of the medium can be expressed by $\rho = \rho^{(0)} + \rho^{(1)}$, $c_{ijkl} = c_{ijkl}^{(0)} + c_{ijkl}^{(1)}$, where the superscript ⁽⁰⁾ denotes a smoothly varying background component and the superscript ⁽¹⁾ denotes a rapidly varying perturbation. As a solution we shall use the geometric ray approximation (GRA) to the Green’s function: $G_{ip}(\mathbf{x}, \mathbf{x}', \omega) = \xi_i(\mathbf{x}) \xi_p(\mathbf{x}') A(\mathbf{x}, \mathbf{x}') \exp[i\omega \tau(\mathbf{x}, \mathbf{x}')$. Here $\tau(\mathbf{x}, \mathbf{x}')$ is the travelttime along the ray connecting \mathbf{x} with \mathbf{x}' . The vectors $\xi_i(\mathbf{x})$ and $\xi_p(\mathbf{x}')$ are the polarization vectors at the endpoints of the ray, and describe the direction of the particle displacement. The polarization vectors are normalized so that $\xi_i \xi_i = 1$. The ray-theoretical displacement amplitude $A(\mathbf{x}, \mathbf{x}')$ is in general a complex quantity that can be expressed in terms of the relative geometrical spreading function and the KMAH index along the ray (Červený, 1995).

A scattering point \mathbf{x} in the subsurface volume \mathcal{D} is connected with a source point \mathbf{s} and a receiver point \mathbf{r} with rays emanating from \mathbf{x} . The slowness vectors associated with the source ray and the receiver ray at \mathbf{x} are

$$\tilde{\boldsymbol{\gamma}}_{\mathbf{x}} = \nabla_{\mathbf{x}}\tau(\mathbf{x}, \mathbf{s}) = \tilde{V}^{-1}\tilde{\boldsymbol{\alpha}}_{\mathbf{x}}, \quad \hat{\boldsymbol{\gamma}}_{\mathbf{x}} = \nabla_{\mathbf{x}}\tau(\mathbf{x}, \mathbf{r}) = \hat{V}^{-1}\hat{\boldsymbol{\alpha}}_{\mathbf{x}}, \quad (1)$$

respectively, where $V(\mathbf{x})$ and $V(\mathbf{x}')$ are the phase velocities and $\tilde{\boldsymbol{\alpha}}_{\mathbf{x}}$ and $\hat{\boldsymbol{\alpha}}_{\mathbf{x}}$ are the associated phase directions as shown in figure 1(a). We shall consider a wave which travels in a given mode from the source to the scattering point, and after a possible mode-conversion, travels further to a receiver point. In the ray-Born approximation, where the wave propagation operators are given by the GRA, the p -component of the scattered wave field due to a q -component point body force at \mathbf{s} is given by (Burridge *et al.*, 1998)

$$U_{pq}^{(1)}(\mathbf{s}, \mathbf{r}, \omega) \simeq (\mathbf{L}\mathbf{c}^{(1)})(\mathbf{s}, \mathbf{r}, \omega) = \omega^2 \int_{\mathcal{D}} \rho^{(0)}(\mathbf{x}) \hat{\xi}_p(\mathbf{r}) A(\mathbf{x}) \tilde{\xi}_q(\mathbf{s}) (\mathbf{w}(\mathbf{s}, \mathbf{x}, \mathbf{r}))^T \mathbf{c}^{(1)}(\mathbf{x}) \exp[i\omega T(\mathbf{x})] d\mathbf{x}, \quad (2)$$

with polarization vectors $\tilde{\xi}$ and $\hat{\xi}$ at the source and receiver, respectively. The relative perturbation in the medium parameters is $\mathbf{c}^{(1)} = \left\{ \frac{\rho^{(1)}}{\rho^{(0)}}, \frac{c_{ijkl}^{(1)}}{\rho^{(0)} \tilde{V}_o \hat{V}_o} \right\}$, where \tilde{V}_o and \hat{V}_o are the local phase velocity of the appropriate modes in the background medium averaged over all phase directions. The notation $_o$ is meant to emphasize that the quantity is angle independent. The point contrast-source ‘radiation pattern’ \mathbf{w} is given by $\mathbf{w} = \left\{ \hat{\xi}_m \tilde{\xi}_m, \hat{V}_o \tilde{V}_o \left[\hat{\xi}_i (\hat{\boldsymbol{\gamma}}_{\mathbf{x}})_j \tilde{\xi}_k (\tilde{\boldsymbol{\gamma}}_{\mathbf{x}})_l \right] \right\}$. In *acquisition* coordinates, we define the total or two-way travel time T for the two rays connecting a source \mathbf{s} with a receiver \mathbf{r} via a scatterer at \mathbf{x} , as $T(\mathbf{r}, \mathbf{x}, \mathbf{s}) = \tau(\mathbf{s}(\mathbf{x}, \tilde{\boldsymbol{\alpha}}_{\mathbf{x}}), \mathbf{x}) + \tau(\mathbf{r}(\mathbf{x}, \hat{\boldsymbol{\alpha}}_{\mathbf{x}}), \mathbf{x})$, and the two-way amplitude becomes $A(\mathbf{x}) = \tilde{A}(\mathbf{x}) \hat{A}(\mathbf{x}) = A(\mathbf{s}(\mathbf{x}, \tilde{\boldsymbol{\alpha}}_{\mathbf{x}}), \mathbf{x}) A(\mathbf{r}(\mathbf{x}, \hat{\boldsymbol{\alpha}}_{\mathbf{x}}), \mathbf{x})$. Finally, we define the gradient of the two-way traveltime at the scattering point $\boldsymbol{\Gamma}_{\mathbf{x}} = \tilde{\boldsymbol{\gamma}}_{\mathbf{x}} + \hat{\boldsymbol{\gamma}}_{\mathbf{x}}$ which, in acquisition coordinates, corresponds to $\boldsymbol{\Gamma}_{\mathbf{x}} = \nabla_{\mathbf{x}} T(\mathbf{r}, \mathbf{x}, \mathbf{s})$.

Imaging-inversion

The inversion is carried out for one image-point \mathbf{y} at a time as an integral over the migration dip vector defined by $\boldsymbol{\nu}_{\mathbf{y}} = \boldsymbol{\Gamma}_{\mathbf{y}}/|\boldsymbol{\Gamma}_{\mathbf{y}}|$. Shooting the rays from \mathbf{y} , we control the initial phase directions and extract a source and a receiver at the surface from the locations where the rays intersect the acquisition surface. The scattering angle θ and azimuth ψ at \mathbf{y} are defined by

$$\cos \theta_{\mathbf{y}} = \tilde{\boldsymbol{\alpha}}_{\mathbf{y}} \cdot \hat{\boldsymbol{\alpha}}_{\mathbf{y}}, \quad \psi_{\mathbf{y}} = \frac{(\tilde{\boldsymbol{\alpha}}_{\mathbf{y}} \cdot \boldsymbol{\nu}_{\mathbf{y}}) \hat{\boldsymbol{\alpha}}_{\mathbf{y}} - (\hat{\boldsymbol{\alpha}}_{\mathbf{y}} \cdot \boldsymbol{\nu}_{\mathbf{y}}) \tilde{\boldsymbol{\alpha}}_{\mathbf{y}}}{\sin \theta_{\mathbf{y}}}. \quad (3)$$

The representation in $\boldsymbol{\nu}_{\mathbf{y}}, \theta_{\mathbf{y}}, \psi_{\mathbf{y}}$ defines a novel coordinate frame, where in terms of acquisition coordinates, the migration dip vector replaces the midpoint and the combination of scattering-angle and azimuth replaces the offset vector. The corresponding angles and phase direction vectors are shown in figure 1(a). In the presence of caustics and multi-pathing, and for a fixed pair $(\theta_{\mathbf{y}}, \psi_{\mathbf{y}})$, the incomplete inverse GRT is given by (Brandsberg-Dahl *et al.*, 2000; De Hoop & Brandsberg-Dahl, 2000)

$$\begin{aligned} M' \mathcal{U}^{(1)}(\mathbf{y}, \theta_{\mathbf{y}}, \psi_{\mathbf{y}}) &\simeq \frac{1}{\pi} \text{Re} \int_0^{\infty} d\omega \frac{1}{8\pi^2} \int_{E_{\boldsymbol{\nu}}(\theta, \psi)} \frac{1}{|E_{\theta} \times E_{\psi}|(\boldsymbol{\nu}_{\mathbf{y}})} \chi_{\{A^{-1} \neq 0\}}(\mathbf{y}, \tilde{\boldsymbol{\alpha}}_{\mathbf{y}}, \hat{\boldsymbol{\alpha}}_{\mathbf{y}}) \\ &\cdot \frac{(-i\omega) |\boldsymbol{\Gamma}_{\mathbf{y}}(\boldsymbol{\nu}_{\mathbf{y}}, \theta_{\mathbf{y}}, \psi_{\mathbf{y}})|^3 |\boldsymbol{\Gamma}_{\mathbf{y}}(\boldsymbol{\nu}_{\mathbf{y}}, \theta_{\mathbf{y}}, \psi_{\mathbf{y}})|}{\rho^{(0)}(\mathbf{y}) A(\mathbf{y}, \boldsymbol{\nu}_{\mathbf{y}}, \theta_{\mathbf{y}}, \psi_{\mathbf{y}}) (\boldsymbol{\nu}_{\mathbf{y}} \cdot \boldsymbol{\nu}_{\phi}(\mathbf{y}))} \\ &\cdot \langle (\mathbf{w}\mathbf{w}^T)(\mathbf{y}, \boldsymbol{\nu}_{\mathbf{y}}, \theta_{\mathbf{y}}, \psi_{\mathbf{y}}) \rangle^{-1} \mathbf{w}(\mathbf{y}, \boldsymbol{\nu}_{\mathbf{y}}, \theta_{\mathbf{y}}, \psi_{\mathbf{y}}) \hat{\xi}_p(\mathbf{r}(\mathbf{y}, \boldsymbol{\nu}_{\mathbf{y}}, \theta_{\mathbf{y}}, \psi_{\mathbf{y}})) \\ &U_{pq}^{(1)}(\mathbf{r}(\mathbf{y}, \boldsymbol{\nu}_{\mathbf{y}}, \theta_{\mathbf{y}}, \psi_{\mathbf{y}}), \mathbf{s}(\mathbf{y}, \boldsymbol{\nu}_{\mathbf{y}}, \theta_{\mathbf{y}}, \psi_{\mathbf{y}}), \omega) \tilde{\xi}_q(\mathbf{s}(\mathbf{y}, \boldsymbol{\nu}_{\mathbf{y}}, \theta_{\mathbf{y}}, \psi_{\mathbf{y}})) \\ &\exp[-i\omega T(\mathbf{y})] d\boldsymbol{\nu}_{\mathbf{y}}, \end{aligned} \quad (4)$$

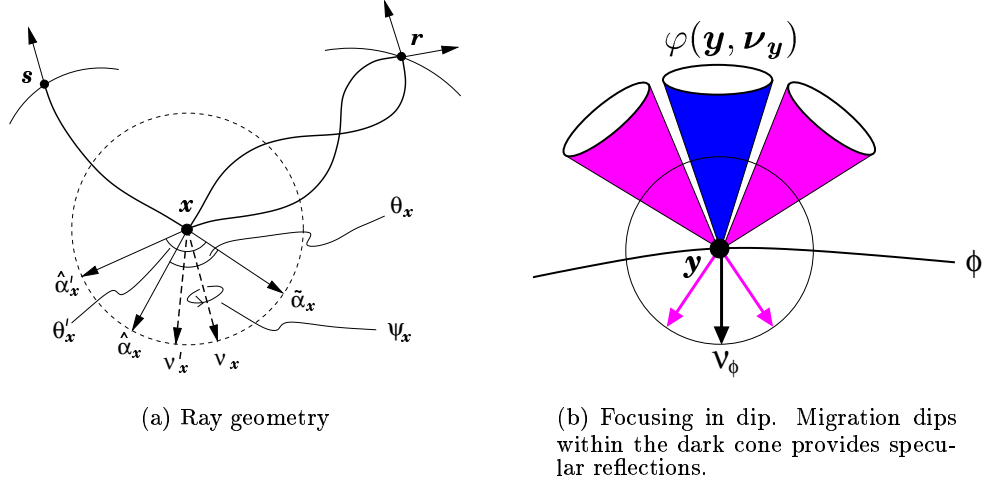


Figure 1: The ray geometry and the conical neighborhoods around the geological dip direction.

The migration dip vector, at the image point, can point in any direction on the unit sphere S^2 . Since any real seismic experiment has limited aperture we cannot expect to have a full or continuous coverage in migration dip. The range of migration dips available will be within some limited domain making up the support E_{ν} of the migration dip. The combination of sources and receivers will dictate the maximum possible coverage of the migration dip, and hence the support is data dependent. Similar limitations hold for the scattering-angle and azimuth domains. The measure is corrected by normalizing with the support of available scattering-angles/azimuths. The factor $|\Gamma_{\mathbf{y}}|^3$ induces a natural taper attenuating contributions over increasingly large scattering-angles, and $\chi_{\{A^{-1} \neq 0\}}$ is a taper function that smoothes the rapid cut off at caustics. The effect of the radiation pattern is removed by applying the generalized inverse $\langle \rangle^{-1}$ of $\mathbf{w}\mathbf{w}^T$, which is calculated through a singular value decomposition in the current background model as a function of position and scattering-angle/azimuth. The outcome of equation (4) is a reconstruction of the medium perturbation for a fixed scattering-angle/azimuth $(\theta_{\mathbf{y}}, \psi_{\mathbf{y}})$.

Focusing in dip

The introduction of the local dip in the inversion procedure allow us to investigate the microlocal behavior of the inversion operator. In the setting described above, where the medium perturbations are localized at, and vary rapidly across interfaces, it is clear that the specular rays will provide the stationary contribution to the integral. After introducing a cutoff function with conically compact support, it will be possible to discriminate dip directions. Let the conical cutoff in the dip domain be $\varphi(\mathbf{y}, \nu_{\mathbf{y}})$. Then the modified ‘measure’ in the inverse operator (4) is $d\nu_{\mathbf{y}} \rightarrow \varphi(\mathbf{y}, \nu_{\mathbf{y}})d\nu_{\mathbf{y}}$, allowing us to perform the inversion for different orientations of the cone φ , see figure 1(b). Whenever the cone is oriented normal to the interface the specular rays will provide the dominant contribution to the integral. If the conical cutoff is oriented with an angle to the interface, non-local and non-stationary contributions will be dominant. This provides a tool to estimate the local geological dip; a procedure which we call ‘focusing in dip’.

Applications

To illustrate some of the features and capabilities of the (incomplete) inverse GRT, we will apply the inversion procedure outlined in the previous sections to a synthetic data example from the gas-cloud model shown in Figure 2(a). The model consists of two layers separated by a ramp-like interface that illustrates a target reflector with an adjacent fault. The upper layer has constant gradients (representative for compaction with depth) in both P -wave and S -wave velocities and density, while the base layer has constant velocities and density. In the upper layer we insert a low P -wave velocity lens with a Gaussian parameter variations to mimic the effect of an overburden gas cloud. The data were generated by a time-domain finite-difference modeling program. Figure 2(b) shows the PP image focused in dip, and a PP CIG with AVA compensation.

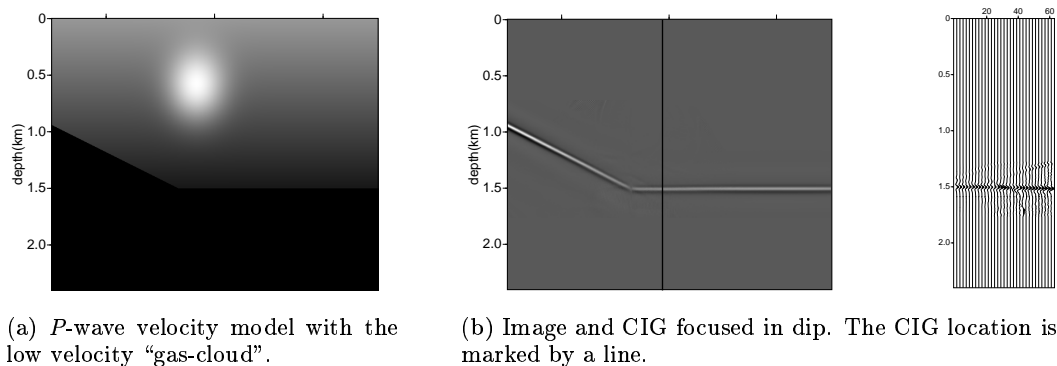


Figure 2: The gas-cloud model.

Conclusions

We have developed a platform of algorithms for velocity analysis, focusing in dip, AVA and imaging in anisotropic elastic media. Our methodology is valid for complex geological settings with formation of caustics and multi-pathing. The outcome of the imaging-inversion is a set of scattering-angle/azimuth common image gathers (CIGs) that are images of points in the subsurface for a range of scattering-angles and azimuths. The CIGs are obtained after conic cut-offs in the migration dip, and thus provide a focusing in dip procedure which also improves the signal-to-noise ratio in the images.

We may compensate for the AVA to pave the way for a differential-semblance-based velocity analysis. This compensation is performed by inverting point-wise for the elastic radiation pattern. Renormalization of the inversion operator is required to be able to interpret the peak amplitudes of coherent events in the gathers. Velocity analysis based on these gathers will be sensitive to errors in traveltme, amplitude and polarization.

Acknowledgments

We thank Sintef Petroleum Research and Ketil Hokstad for generating the finite-difference data for the gas-cloud model. SBD thanks BP Norway and The Norwegian Research Council for financial support.

References

- Brandsberg-Dahl, S., De Hoop, M.V., & Ursin, B. 2000. Focusing in dip and AVA compensation on scattering-angle/azimuth gathers. *submitted to Geophysics*.
- Burridge, R., De Hoop, M. V., Miller, D., & Spencer, C. 1998. Multiparameter inversion in anisotropic media. *Geophys. J. Int.*, **134**, 757–777.
- Castagna, J.P., & Backus, M. M. 1993. *Offset-dependent reflectivity - Theory and practice of AVO analysis*. Tulsa: Soc. Explor. Geophys.
- Červený, V. 1995. *Seismic wave fields in three-dimensional isotropic and anisotropic structures*. Lecture Notes, Norwegian University of Science and Technology, Trondheim.
- De Hoop, M. V., & Brandsberg-Dahl, S. 2000. Maslov extension of generalized Radon transform inversion in anisotropic elastic media:A least-squares approach. *Inverse Problems*, 1–44.
- Jeannot, J.P., Faye, J.P., & Denelle, E. 1986. Pre-stack migration velocities from depth focusing analysis. *In: Expanded Abstracts*. Soc. Explor. Geophys.
- Ursin, B., Ekren, B., & Tjåland, E. 1996. Linearized elastic parameter sections. *Geophysical Prospecting*, **44**, 427–456.